



OPEN ACCESS

EDITED BY
Wenjie Sui,
Tianjin University of Science and
Technology, China

REVIEWED BY
Wei Jiang,
Technical University of
Denmark, Denmark
Xueping Song,
Guangxi University, China

*CORRESPONDENCE
Zhi-Min Zhao
zmzhao@imu.edu.cn

†These authors have contributed
equally to this work and share first
authorship

SPECIALTY SECTION
This article was submitted to
Nutrition and Food Science
Technology,
a section of the journal
Frontiers in Nutrition

RECEIVED 22 August 2022
ACCEPTED 06 September 2022
PUBLISHED 27 September 2022

CITATION
Li C, Zhao K, Ma L, Zhao J and
Zhao Z-M (2022) Effects of drying
strategies on sporulation and titer of
microbial ecological agents with
Bacillus subtilis.
Front. Nutr. 9:1025248.
doi: 10.3389/fnut.2022.1025248

COPYRIGHT
© 2022 Li, Zhao, Ma, Zhao and Zhao.
This is an open-access article
distributed under the terms of the
Creative Commons Attribution License
(CC BY). The use, distribution or
reproduction in other forums is
permitted, provided the original
author(s) and the copyright owner(s)
are credited and that the original
publication in this journal is cited, in
accordance with accepted academic
practice. No use, distribution or
reproduction is permitted which does
not comply with these terms.

Effects of drying strategies on sporulation and titer of microbial ecological agents with *Bacillus subtilis*

Chonglei Li^{1,2†}, Kai Zhao^{1,2†}, Litong Ma³, Ji Zhao¹ and
Zhi-Min Zhao^{1,2*}

¹Inner Mongolia Key Laboratory of Environmental Pollution Control and Wastes Reuse, School of Ecology and Environment, Inner Mongolia University, Hohhot, China, ²Key Laboratory of Ecology and Resource Use of the Mongolian Plateau (Ministry of Education), Inner Mongolia University, Hohhot, China, ³Inner Mongolia Engineering Research Center of Comprehensive Utilization of Bio-coal Chemical Industry, School of Chemistry and Chemical Engineering, Inner Mongolia University of Science and Technology, Baotou, China

Drying operation is beneficial to the preservation and transportation of microbial ecological agents. In this study, drying kinetics and water distribution variations in solid biomass medium during hot air drying (HAD) and vacuum freeze drying (VFD) were systematically investigated. Meanwhile, the effects of different drying strategies on the sporulation of *Bacillus subtilis* and the titer of microbial ecological agents were compared. The results showed that both HAD and VFD induced rapid water removal from the solid biomass medium. VFD retained bound water and maintained the porous structure of the solid medium. Both HAD and VFD induced sporulation. The expression level of sporulation-regulatory genes *spo0A*, *sigF*, and *sigE* followed the order 80°C-HAD > 60°C-HAD > VFD. The spore number in the medium after 80°C-HAD drying for 6 h was 0.72×10^{10} /g dry medium, which was 9.1 and 12.5% larger than that of the medium with 60°C-HAD and VFD, respectively. Therefore, 80°C-HAD is an effective drying strategy for promoting sporulation, which improves the titer of microbial ecological agents with *B. subtilis*.

KEYWORDS

microbial ecological agents, *Bacillus subtilis*, sporulation, hot air drying, vacuum freeze drying, low-field nuclear magnetic resonance

Introduction

The indiscriminate use of antibiotics leads to the occurrence of antibiotic resistance genes (ARGs) and antibiotic-resistant bacteria (ARB) from environments (1, 2). *Bacillus subtilis* microbial ecological agents are environmentally friendly alternatives to antibiotics, which can be utilized as feed additives for preventing disease and promoting animal growth (3–5). The preparation process of microbial ecological agents consists of strain breeding, fermentation, and drying processes, among which the drying process aims to reduce water content (WC) in the solid substrate and enhance the stability of probiotics products for preservation and transportation (6, 7). Hot air

drying (HAD) is widely used for the production of dehydrated food and solid medium. Vacuum freeze-drying (VFD) method sublimates water at subfreezing temperatures. It is the preferred drying method for biomaterials because most biomaterials are vulnerable to heat (8). However, there was rare information about the effects of HAD and VFD on the sporulation and titer of *B. subtilis* microbial ecological agents.

Low-field nuclear magnetic resonance (LF-NMR) has been regarded as a powerful tool to analyze the water states and distribution in the solid medium due to its fast analysis speed, good sensitivity, and non-invasiveness (9, 10). Using the LF-NMR technique, Li et al. (11) identified three different proton fractions (T_{2b} , T_{21} , and T_{22}) with various mobilities in the glutinous rice during solid-state fermentation (SSF). Recently, the LF-NMR technique has exhibited an excellent ability to explore the water dynamics during the drying process for solid substrates (12). Bacteria spore number is a key indicator to evaluate the quality of microbial ecological agents (13). By forming spores, bacteria cells can survive in severe environments (e.g., acid and mechanical force) and reawaken when favorable conditions return (14). Spores of *B. subtilis* are resistant to environmental stress, which includes heat in the drying process (15). The sporulation process begins with the activation of the master transcriptional gene *spo0A*, which leads to the sequential activation of the *sigF* gene in the forespore and the *sigE* gene in the parent cell (16). Therefore, the expression of *spo0A*, *sigF*, and *sigE* genes can indicate the sporulation process of *B. subtilis* with different drying strategies.

This study aimed to compare the effects of different drying strategies on the sporulation of *B. subtilis* and improved the titer of microbial ecological agents. The key metrics, such as water dynamics, molecular genetic expressions, viable cell, and spore number variations, were systematically evaluated and compared. These together could help to reveal the relationship between water distribution and sporulation during different drying processes, which could further benefit the production of microbial ecological agents of *B. subtilis*.

Materials and methods

Solid-state fermentation

Bacillus subtilis 10732 was purchased from the China Center of Industrial Culture Collection (CICC). The strain was stored in Luria-Bertani (LB) medium slant at 4°C. *B. subtilis* 10732 was precultivated in 100 ml of a liquid medium that contained 1% (w/w) yeast extract, 4% (w/w) glucose, 1% (w/w) peptone, 1% (w/w) CaCO₃, and 0.05% (w/w) MgSO₄ at 37°C and was shaken at 150 rpm for 24 h.

The solid medium consisted of 3.0 g of soybean meal, 30 g wheat bran, 0.75 g glucose, 1.5 g CaCO₃, 30 ml of 1.25% (w/w) (NH₄)₂SO₄, 0.05% (w/w) MnSO₄, 2.5% (w/w) KH₂PO₄

inorganic salt solution, and 9.6 ml of deionized water. The medium was put into 250 ml Erlenmeyer flasks and sterilized at 121°C for 20 min. Afterward, the medium was cooled at room temperature and then inoculated by adding 12 ml of seed solution. The fermentation was conducted in an incubator at 37°C for 72 h.

Drying experiment

After fermentation, the solid medium was subjected to different drying treatments. The solid biomass medium was dehydrated until reaching constant weight. The temperatures of HAD were set at 60 and 80°C. The process of VFD included two steps: freezing and drying. All water in the solid medium was frozen in the first freezing step at -80°C for 1 h. The drying step was set at -45°C and 10 Pa to remove water in a vacuum environment until the medium reached a constant weight (8, 17).

Water content and drying rate (DR) are two important indicators to reveal the drying performance (12, 18). During the drying process, the mass of the solid medium was weighed, and the WCs (dry basis, g·g⁻¹) were calculated using Equation (1):

$$WC_t = (m_t - m_e)/m_e \quad (1)$$

where WC_t is the WC (g·g⁻¹) at the time t , m_t is the mass (g) of the solid medium at t h, and m_e is the final dry mass (g) of the solid medium. DR (g·g⁻¹·h⁻¹) was calculated according to Equation (2):

$$DR = (WC_t - WC_{t+\Delta t})/\Delta t \quad (2)$$

where WC_t and $WC_{t+\Delta t}$ are the WC at t and $t + \Delta t$, respectively. The samples were taken at intervals of 1 h for WC and DR analyses.

LF-NMR measurements

Low-field nuclear magnetic resonance was applied to analyze water states and dynamics in a solid medium on a MesoMR23-060H-I Analyst Analyzing and Imaging System (Niumag Co., Ltd., Shanghai, China). In total, 2.60 g of solid medium samples were obtained from the central part of the substrates. The samples were placed into 25 mm NMR glass tubes first and then inserted into the NMR probe for detection. The T_{2j} relaxation times were measured using Carr-Purcell-Meiboom-Gill (CPMG) sequence with a τ -value of 100 μ s. A total of 3,000 echoes were collected as 16 scan repetitions, and the repetition time between two successive scans was 2.5 s. The relaxation time measurements were performed at 32°C. Data

analysis was performed with the NMR Analyzing System version 1.0 (Niumag Co., Ltd., Shanghai, China). Relaxation time T_{2i} and its corresponding water proportion M_{2i} were presented.

Measurement of viable cell and spore number

Approximately 3 g of the solid medium was mixed with sterile water (1:20, w/v) in a 250 ml Erlenmeyer flask and shaken at 150 rpm for 30 min at 37°C. In total, 100 μ l of the supernatant was carefully sampled and serially diluted (10^6 -fold). Afterward, the cell count was determined by the spread plate method on LB plates. After incubation at 37°C for 24 h, the viable cell number was counted and expressed as colony-forming units (CFUs). Similarly, 5.0 ml of the mixture after shaking at 150 rpm for 30 min at 37°C in the determination of viable cell number was sampled and cultured at 80°C for 15 min. Afterward, 100 μ l of the mixture was serially diluted (10^6 -fold) and spread on LB plates. After incubation at 37°C for 24 h, the spore number was determined.

Quantitative polymerase chain reaction (qPCR) analysis of *spo0A*, *sigF*, and *sigE* gene expressions

Approximately 1 g of the solid medium was sampled and mixed with sterile water (1:20, w/v) in a 50 ml sterile test tube and shaken at 150 rpm for 5 min. Afterward, the mixture was centrifuged at 8,000 rpm for 10 min, and the precipitate was separated and stored at -80°C . Total RNA of *B. subtilis* was extracted using Cetyltrimethylammonium Bromide (CTAB) method (19). Before reverse transcription, the purity of the total RNA was tested by measuring OD260 and OD280 with a Nano Photometer P-Class P360 Ultraviolet Spectrophotometer. In total, 10 μ l of total RNA was used as a template and was reverse transcribed to cDNA using PrimeScript RT Regent Kit (Takara Company) with a final volume of 20 μ l. Moreover, the mixture was incubated at 37°C for 15 min and then at 85°C for 5 min to inactivate the enzyme. The primers for qPCR were synthesized by Sangon Biotech (Shanghai, China). The qPCR procedure was 30 s at 95°C followed by 35 cycles of 30 s at 95°C, 45 s at the annealing temperature of 35°C, and 45 s at 72°C, with a melt curve increasing from 65 to 95°C at increments of 0.5°C. The sample dried for 0 h was selected as the calibration sample for the gene expressions of *spo0A*, *sigF*, and *sigE*. The relative quantification of gene transcription was analyzed using the $2^{-\Delta\Delta\text{Ct}}$ method (20).

Statistical analysis

Statistical analysis was performed by using SPSS version 21.0. Differences between the means were evaluated by the one-way ANOVA and the independent samples *t*-tests.

Results and discussion

Changes of WC and DR during different drying processes

Water content and DR are two important indicators to evaluate the drying process of a solid medium. Effects of different drying strategies on WC and DR were investigated (Figure 1). The WC of all media was decreased during the drying processes. The solid medium reached constant weight after 4 h drying with 80°C-HAD, while the time needed to reach constant weight with VFD and 60°C-HAD was 5 and 6 h, respectively. The higher the drying temperature, the faster the WC of the solid medium declined (12). Figure 1B shows that DR of 80°C-HAD and VFD increased from 0 to 1 h and then decreased gradually to the end of the drying process. The maximum DR values of 80°C-HAD and VFD were 0.60 and 0.72 $\text{g}\cdot\text{g}^{-1}\cdot\text{h}^{-1}$, respectively. The highest DR of 60°C-HAD was 0.45 $\text{g}\cdot\text{g}^{-1}\cdot\text{h}^{-1}$, which appeared during the period of 1–2 h. Sun et al. (18) reported that there were three stages during microwave freeze-drying for raspberry: the speed-up drying stage (I), the speed-down drying stage (II), and the low-speed drying stage (III), respectively. In line with the previous study, the drying process of solid biomass medium with HAD and VFD in this study could also be divided into three periods: (I) the speed-up drying period (0–1 h for 80°C-HAD and VFD and 0–2 h for 60°C-HAD); (II) the speed-down drying period (1–4 h for 80°C-HAD and VFD and 2–4 h for 60°C-HAD); and (III) the low-speed drying stage (4–8 h for 60°C-HAD, 80°C-HAD, and VFD). In the drying period I, the solid biomass medium presented higher WC and stronger heat absorption ability as compared to periods II and III, which caused the rapid water removal (7). With the extension of drying, the WC and heat absorption capacity of the medium were decreased. Meanwhile, the change in the internal structure of the solid medium also inhibited the water distribution (18), which was responsible for the DR decrease.

Comparison of water state variations of solid media during different drying processes

Low-field nuclear magnetic resonance can be used to evaluate water states in the substrate, which are significantly related to the microstructure of the solid medium (21). In this study, water dynamics and relaxation times of T_{2i} fractions

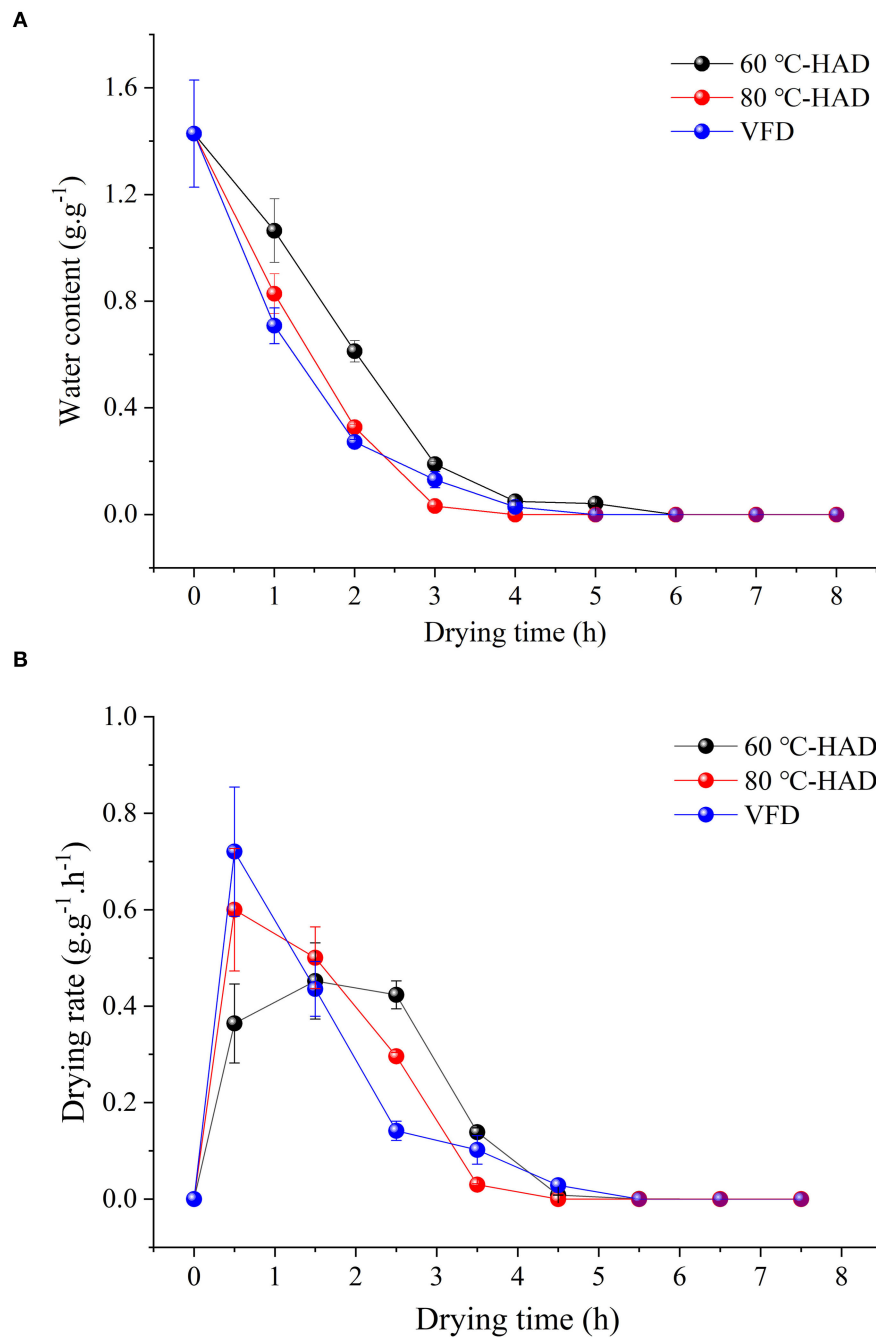


FIGURE 1
Changes in water content (A) and drying rate (B) during different drying processes.

were investigated to elucidate the microstructure changes of solid medium treated by different drying strategies. Figure 2 shows that three kinds of proton fractions are found in the solid medium after fermentation (curve at 0 h). The different fractions represent three different states of water, namely, (1)

bound water, T_{2b} associated with hydroxyl and/or carboxyl hydrophilic groups (22); (2) capillary water, T_{21} attributed to the water molecules in pores of solid media (23); and (3) lumen water, T_{22} ascribed to water molecules in the cavities of the three-dimensional network in solid media (11). M_{2b} , M_{21} , and

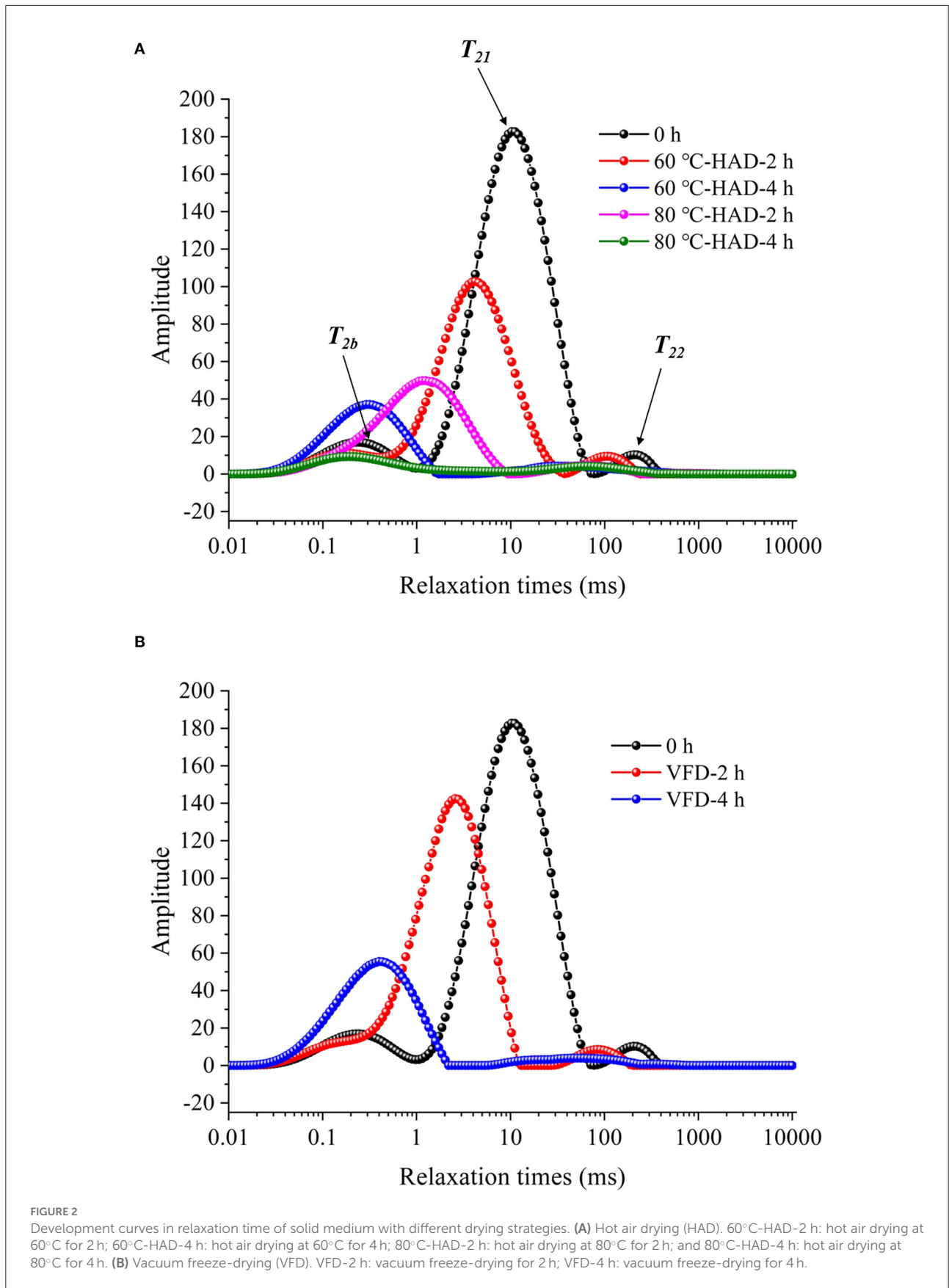


TABLE 1 Relaxation times (T_{2i}) and water proportion (M_{2i}) of the solid biomass medium during drying processes.

T_{2i} and M_{2i} Drying condition	T_{2b} (ms)	T_{21} (ms)	T_{22} (ms)	M_{2b} (Peak area/a.u.)	M_{21} (Peak area/a.u.)	M_{22} (Peak area/a.u.)	$\sum M_{2i}$ (Peak area/a.u.)
0 h	0.25	11.10	240.94	408	4630	125	5163
60°C-HAD-2h	0.16	4.20	107.19	250	2701	65	3016
60°C-HAD-4h	0.29	34.49 ($T_{21}T_{22}M$)		1023	140 ($M_{21}M_{22}M$)		1163
80°C-HAD-2h	1.15	65.93 ($T_{21}T_{22}M$)		1617	107 ($M_{21}M_{22}M$)		1724
80°C-HAD-4h	0.21	65.93 ($T_{21}T_{22}M$)		313	115 ($M_{21}M_{22}M$)		428
VFD-2h	2.58 ($T_{2b}T_{21}M$)		84.07	3842 ($M_{2b}M_{21}M$)		116	3958
VFD-4h	0.40	51.71 ($T_{21}T_{22}M$)		1601	132 ($M_{21}M_{22}M$)		1733

$T_{21}T_{22}M$: T_{21} and T_{22} merged; $T_{2b}T_{21}M$: T_{2b} and T_{21} merged; $M_{21}M_{22}M$: M_{21} and M_{22} merged; $M_{2b}M_{21}M$: M_{2b} and M_{21} merged; $\sum M_{2i}$ is the sum of M_{2b} , M_{21} , and M_{22} .

M_{22} were the corresponding water proportion, respectively. Table 1 shows that the T_{2b} , T_{21} , and T_{22} relaxation times and M_{2b} , M_{21} , and M_{22} water proportions are decreased during 60°C-HAD for 2 h, which indicates the reduction of water fluidity and a decrease of WC. T_{21} capillary water and T_{22} lumen water were the relatively free water in solid biomass medium, which can be removed first in the drying process. However, T_{2b} bound water was associated with hydroxyl and/or carboxyl hydrophilic groups, which was relatively difficult to remove. It should be noted that T_{21} and T_{22} peaks were merged into 1 weak peak at 60°C-HAD-4 h, 80°C-HAD-2 h, 80°C-HAD-4 h, and VFD-4 h conditions. T_{2b} and T_{21} peaks were merged into 1 weak peak at VFD-2 h. It was speculated that drying treatments can break the barriers between different water fractions, thereby leading to the merging of T_{21} and T_{22} and T_{2b} and T_{21} peaks. Tang et al. (24) also reported that water fractions can only be distinguished where microstructural barriers exist because they can hinder the inter-compartment water diffusion, which was consistent with the present results.

The $\sum M_{2i}$ of the solid medium at 80°C-HAD-2 h decreased by 42.8% than that at 60°C-HAD-2 h, while the $\sum M_{2i}$ at 80°C-HAD-4 h decreased by 63.2% than that at 60°C-HAD-4 h. These results indicated that the higher drying temperature during HAD could accelerate the water release from the medium. The proportion of M_{2b} to $\sum M_{2i}$ at VFD-4 h was 92.4%, which was higher than that of 60°C-HAD and 80°C-HAD at the same drying time. VFD is a process in which water is crystallized at a low temperature and thereafter sublimated from the solid state directly into the vapor phase (25). The capillary water and lumen water were frozen as ice crystals and sublimated, but the bound water was retained with VFD. In summary, both HAD and VFD decreased the water fraction amplitudes and altered the water fraction distributions within a solid biomass medium. These different water states within the media should influence the sporulation process of *B. subtilis*.

Expression of sporulation-regulatory genes during different drying processes

The expression of *spo0A*, *sigF*, and *sigE* genes associated with sporulation during the drying processes was systematically investigated. Figure 3A shows that the expression of the *spo0A* gene exhibited an increasing tendency with the extension of drying time. Since the *spo0A* gene is the major regulator for the initiation of sporulation (26, 27), the increasing expression of *spo0A* illustrated the enhanced sporulation process with the HAD and VFD drying strategies. After drying for 6 h, the expression of the *spo0A* gene in 80°C-HAD reached 2.8, which was higher than that of 60°C-HAD (1.8) and VFD (1.8). It suggested that the 80°C-HAD drying strategy can facilitate the sporulation process more significantly.

As seen in Figures 3B,C, the expression of *sigF* and *sigE* genes in 80°C-HAD is increased by 206 and 249% from 0 to 6 h drying time, respectively. The expression of *sigF* and *sigE* genes in 60°C-HAD was increased by 70 and 120% from 0 to 6 h drying time, respectively. The expression of *sigF* and *sigE* genes in VFD increased by 10 and 100% from 0 to 6 h drying time, respectively. These results showed that the *sigF* and *sigE* genes exhibited increasing tendencies with the extension of drying time, which were similar to the *spo0A* gene expression variation. The expression levels of *sigF* and *sigE* gene at 80°C-HAD after 6 h drying were 1.76 and 1.57 times of those at 60°C-HAD. Fimlaid et al. (28) reported that the *sigF* and *sigE* genes are expressed in a *spo0A*-dependent manner. The higher the drying temperature, the more intense the sporulation process. Activation of the master transcriptional gene *spo0A* leads to the sequential activation of *sigF* and *sigE* genes, which can activate compartment-specific transcriptional programs that drive sporulation through its morphological stages (16). Both HAD and VFD induced sporulation. The expressions of *spo0A*, *sigF*, and *sigE* genes during drying followed the order 80°C-HAD > 60°C-HAD > VFD. These results indicated that high temperature in HAD facilitated sporulation-regulatory gene

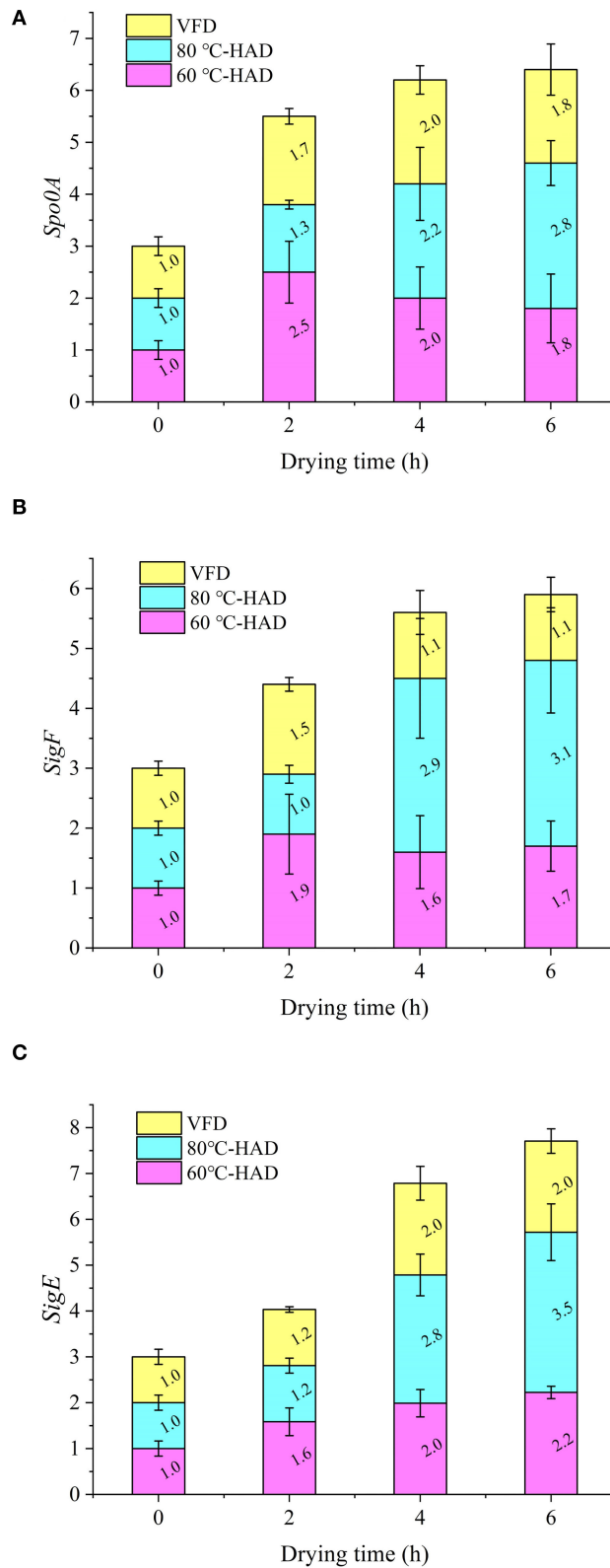
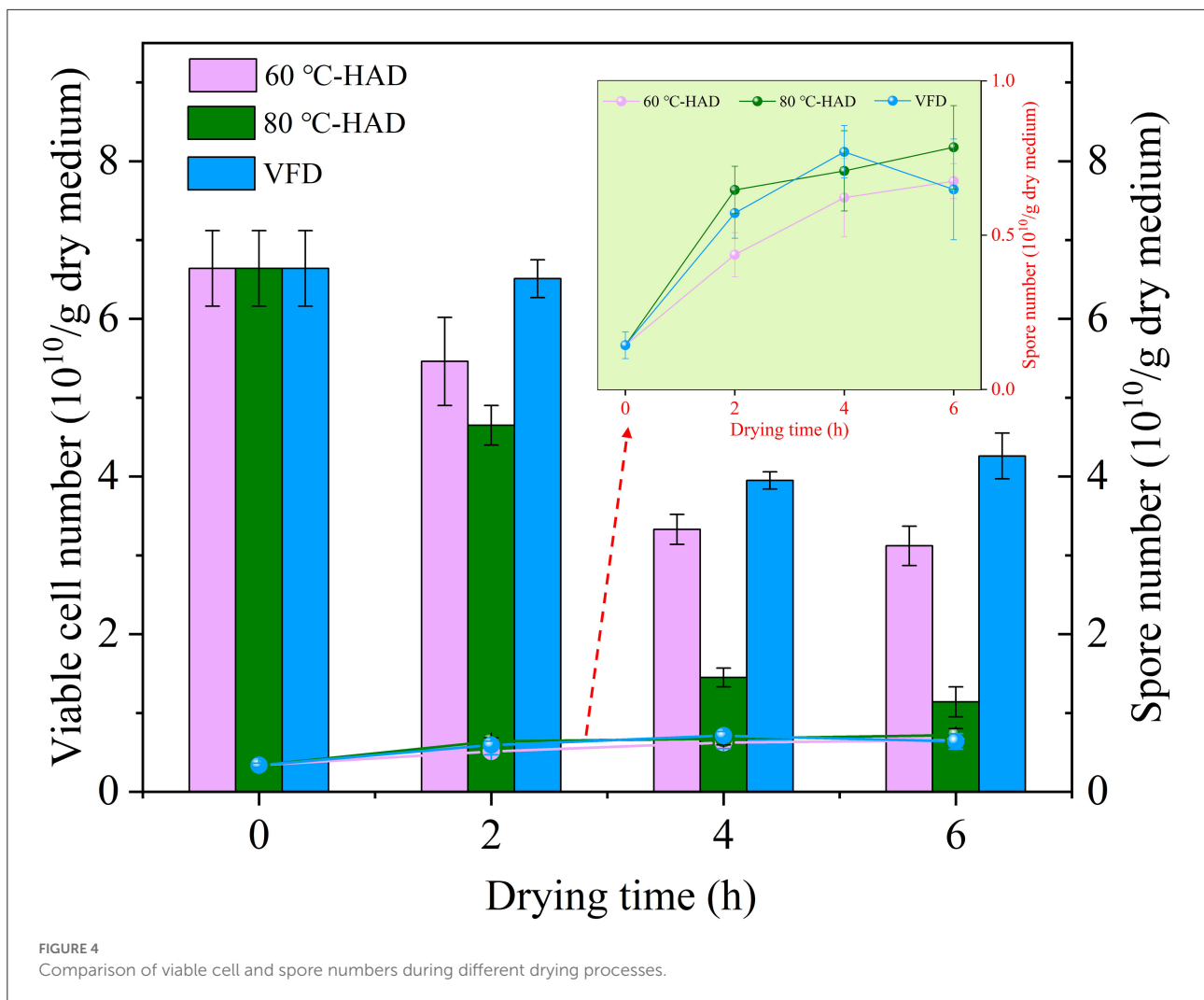


FIGURE 3
Expressions of *spo0A* (A), *sigF* (B), and *sigE* (C) genes during different drying processes.



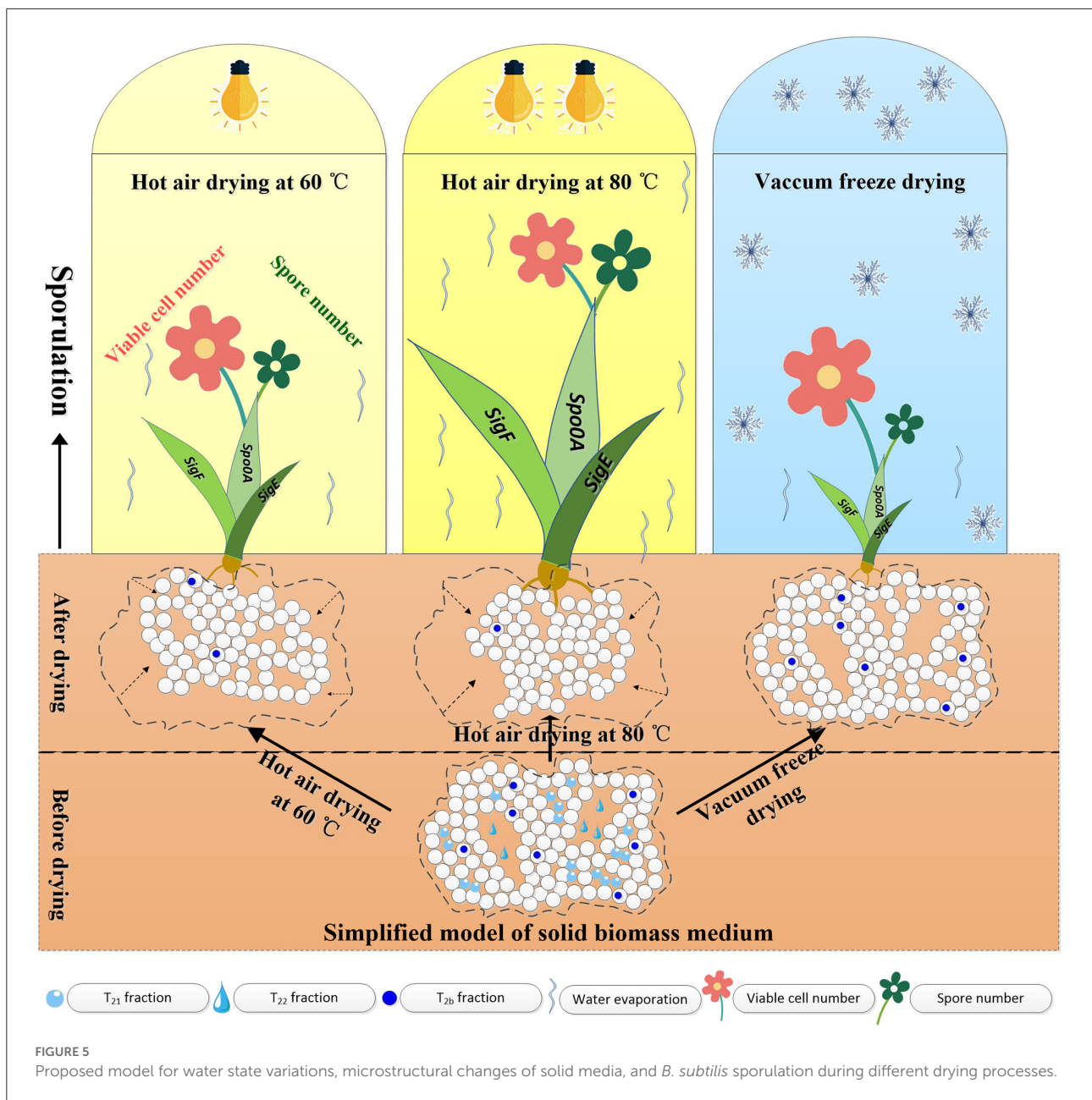
expression, which was more likely to promote sporulation of *B. subtilis*.

Viable cell and spore number changes during different drying processes

The number of viable cells and spores can be used to evaluate the quality of microbial ecological agents, food additives, etc. (13, 29, 30). Figure 4 shows the variation of viable cell and spore numbers in media with different drying strategies. The viable cell number exhibited decreasing tendencies, while the spore number showed increasing trends with the extension of drying time in all media. It should be noted that the viable cell number decreased fast while the spore number increased rapidly from 0 to 4 h in 80°C-HAD, 60°C-HAD, and VFD processes. The possible reason for this phenomenon was that WC decreased

fast during this drying period. Influenced by the rapid removal of water, the viable cell formed spores to resist harsh environments.

With the extension of drying time, the viable cell number of 80°C-HAD was always lower than that of 60°C-HAD, while the spore number of 80°C-HAD was always higher than that of 60°C-HAD. Especially, the viable cell numbers of 80°C-HAD at 4 and 6 h drying time were 1.45×10^{10} and 1.14×10^{10} /g dry medium, respectively, which were lower than that of 60°C-HAD at 4 h (3.33×10^{10} /g dry medium) and 6 h (3.12×10^{10} /g dry medium). Moreover, the 80°C-HAD strategy caused a more rapid water decrease in the solid medium than 60°C-HAD, resulting in a more hydropenic environment. This severe condition induced more viable cell death or transformation to spores under 80°C-HAD. Previous studies reported that air drying caused physical alterations (e.g., shrinkage), which decreased the porosity of the microscopic structure of substrate materials (31–33). Similarly, HAD in the present study also led to the shrinkable structure of solid biomass medium with the



extension of drying. The inferior porosity of the solid biomass medium was harmful to the growth of vegetative cells, which enhanced sporulation. The spore number of 80°C-HAD was $0.72 \times 10^{10}/g$ dry medium after 6 h of drying, which was 9.1 and 12.5% larger than that of 60°C-HAD and VFD, respectively. The spore number of 80°C-HAD, 60°C-HAD, and VFD was increased by 115, 95, and 90%, respectively, during 0–6 h drying processes. Therefore, it can be concluded that the drying processes in the present study promoted sporulation. It should also be noted that the viable cell number of VFD showed a slight increase while the spore number decreased slightly during drying for 4–6 h. This phenomenon was contrary to the general

trend of viable cell and spore numbers but can be explained by the specific sublimation drying process of VFD. By drying in the frozen state, the free water fractions within the solid medium were presented as ice crystals. Then, these water fractions were sublimated continuously with the extension of drying time (25). As a result, the pores and cavities were vacated in the final period of drying, providing a porous medium and effective contact space for spore germination during 4–6 h drying time. Overall, VFD can maintain the porous structure of a solid medium, but HAD, especially 80°C-HAD, presented the vigorous sporulation process, which improved the titer of microbial ecological agents with *B. subtilis*.

Based on the above experimental results, a comprehensive model was proposed to elucidate the water state variations, microstructural changes of solid media, and *B. subtilis* sporulation during different drying processes. As seen in Figure 5, HAD leads to the shrinkage of pores and cavities in solid media, but VFD retains bound water and maintains the porous structure. Both HAD and VFD induced sporulation. The expression levels of *spo0A*, *sigF*, and *sigE* genes with 80°C-HAD were the highest as compared to 60°C-HAD and VFD, resulting in the largest spore number in medium with 80°C-HAD. The proposed model clearly elucidated the water states and microstructure changes within solid biomass media, which provided a better understanding of the effects of drying strategies on the sporulation of *B. subtilis*.

Conclusion

Effects of different drying strategies on the sporulation of *B. subtilis* were revealed. Both HAD and VFD induced rapid water removal from solid biomass medium and facilitated sporulation. The expression level of sporulation-regulatory genes followed the order 80°C-HAD > 60°C-HAD > VFD. Accordingly, the spore number with 80°C-HAD was increased by 9.1 and 12.5% than that of 60°C-HAD and VFD, respectively. Therefore, 80°C-HAD is an effective drying strategy for promoting sporulation, which improves the titer of *B. subtilis* microbial ecological agents effectively.

Data availability statement

The original contributions presented in the study are included in the article/supplementary material, further inquiries can be directed to the corresponding author/s.

References

- Guan AM, Qi WX, Peng Q, Zhou JM, Bai YH, Qu JH. Environmental heterogeneity determines the response patterns of microbially mediated N-reduction processes to sulfamethoxazole in river sediments. *J Hazard Mater.* (2021) 11:126730. doi: 10.1016/j.jhazmat.2021.126730
- Barrios RE, Khuntia HK, Bartelt-Hunt SL, Gilley JE, Schmidt AM, Snow DD, Li X. Fate and transport of antibiotics and antibiotic resistance genes in runoff and soil as affected by the timing of swine manure slurry application. *Sci Total Environ.* (2020) 712:136505. doi: 10.1016/j.scitotenv.2020.136505
- Pan X, Cai YL, Kong LL, Xiao CP, Zhu QD, Song ZG. Probiotic effects of *Bacillus licheniformis* DSM5749 on growth performance and intestinal microecological balance of laying hens. *Front Nutr.* (2022) 9:868093. doi: 10.3389/fnut.2022.868093
- Kaspar F, Neubauer P, Gimpel M. Bioactive secondary metabolites from *Bacillus subtilis*: a comprehensive review. *J Nat Prod.* (2019) 82:7. doi: 10.1021/acs.jnatprod.9b00110
- Gao DY, Sun XB, Liu MQ, Liu YN, Zhang HE, Shi XL, et al. Characterization of thermostable and chimeric enzymes via isopeptide bond-mediated molecular cyclization. *J Agr Food Chem.* (2019) 67:6837–46. doi: 10.1021/acs.jafc.9b01459
- Chen H, Chen SW, Li CN, Shu GW. Response surface optimization of lyoprotectant for *Lactobacillus bulgaricus* during vacuum freeze-drying. *Prep Biochem Biotech.* (2015) 45:463–75. doi: 10.1080/10826068.2014.923451
- Ambros S, Mayer R, Schumann B, Kulozik U. Microwave-freeze drying of lactic acid bacteria: Influence of process parameters on drying behavior and viability. *Innov Food Sci Emerg.* (2018) 48:90–8. doi: 10.1016/j.ifset.2018.05.020
- Byun SY, Kang JS, Chang YS. Analysis of primary drying of poly- γ -glutamic acid during vacuum freeze drying. *J Mech Sci Technol.* (2020) 34:4323–32. doi: 10.1007/s12206-020-0922-9
- Kirtil E, Oztop MH. ¹H nuclear magnetic resonance relaxometry and magnetic resonance imaging and applications in food science and processing. *Food Eng Rev.* (2015) 8:1–22. doi: 10.1007/s12393-015-9118-y
- Kirtil E, Cikrikci S, McCarthy MJ, Oztop MH. Recent advances in time domain NMR & MRI sensors and their food applications. *Curr Opin Food Sci.* (2017) 17:9–15. doi: 10.1016/j.cofs.2017.07.005
- Li T, Tu C, Rui X, Gao Y, Li W, Wang K, et al. Study of water dynamics in the soaking, steaming, and solid-state fermentation of glutinous rice by

Author contributions

Conceptualization: Z-MZ. Formal analysis: CL, KZ, and Z-MZ. Funding acquisition: Z-MZ and LM. Investigation: KZ, CL, and Z-MZ. Project administration: Z-MZ and JZ. Writing—original draft: CL and KZ. Writing—review and editing: CL, KZ, LM, JZ, and Z-MZ. All authors contributed to the article and approved the submitted version.

Funding

This work was supported by the National Natural Science Foundation of China (Grant Numbers 21706136 and 21766025) and the Natural Science Foundation of Inner Mongolia (Grant Number 2019MS02026).

Conflict of interest

The authors declare that the research was conducted in the absence of any commercial or financial relationships that could be construed as a potential conflict of interest.

Publisher's note

All claims expressed in this article are solely those of the authors and do not necessarily represent those of their affiliated organizations, or those of the publisher, the editors and the reviewers. Any product that may be evaluated in this article, or claim that may be made by its manufacturer, is not guaranteed or endorsed by the publisher.

- LF-NMR: a novel monitoring approach. *J Agr Food Chem.* (2015) 63:3261–70. doi: 10.1021/acs.jafc.5b00769
12. Cheng SS, Li RR, Yang HM, Wang SQ, Tan MQ. Water status and distribution in shiitake mushroom and the effects of drying on water dynamics assessed by LF-NMR and MRI. *Dry Technol.* (2020) 38:1001–10. doi: 10.1080/07373937.2019.1625364
 13. Veen B, Xie H, Esveld E, Abee T, Mastwijk H, Groot MN. Inactivation of chemical and heat-resistant spores of *Bacillus* and *Geobacillus* by nitrogen cold atmospheric plasma evokes distinct changes in morphology and integrity of spores. *Food Microbiol.* (2015) 45:26–33. doi: 10.1016/j.fm.2014.03.018
 14. Setlow P, Johnson EA. Spores and their significance. *Food Microbiol Fundam Front.* (2019) 23–63. doi: 10.1128/9781555819972.ch2
 15. Zhao ZM, Xi JT, Xu JF, Ma LT, Zhao J. Enhancement of *Bacillus subtilis* growth and sporulation by two-stage solid-state fermentation strategy. *Processes.* (2019) 7:644. doi: 10.3390/pr7100644
 16. Tan IS, Ramamurthi KS. Spore formation in *Bacillus subtilis*. *Env Microbiol Rep.* (2014) 6:212–25. doi: 10.1111/1758-2229.12130
 17. Patel SM, Doen T, Pikal MJ. Determination of end point of primary drying in freeze-drying process control. *AAPS PharmSciTech.* (2010) 11:73–84. doi: 10.1208/s12249-009-9362-7
 18. Sun Y, Zhang M, Mujumdar AS, Yu D. Pulse-spouted microwave freeze drying of raspberry: control of moisture using ANN model aided by LF-NMR. *J Food Eng.* (2021) 292:110354. doi: 10.1016/j.jfoodeng.2020.110354
 19. Farrag M, Abri S, Leipzig ND. pH-dependent RNA isolation from cells encapsulated in chitosan-based biomaterials. *Int J Biol Macromol.* (2020) 146:422–30. doi: 10.1016/j.ijbiomac.2019.12.263
 20. Hong Y, Zhou Z, Yu LZ, Jiang KY, Xia JM, Mi YL, Zhang CQ, Li J. *Lactobacillus salivarius* and *Lactobacillus agilis* feeding regulates intestinal stem cells activity by modulating crypt niche in hens. *Appl Microbiol Biot.* (2021) 105:8823–35. doi: 10.1007/s00253-021-11606-2
 21. Liu ZH, Chen HZ. Biomass-water interaction and its correlations with enzymatic hydrolysis of steam-exploded corn stover. *ACS Sustain Chem Eng.* (2016) 4:1274–85. doi: 10.1021/acssuschemeng.5b01303
 22. Li T, Rui X, Li W, Chen XH, Jiang M, Dong MS. Water distribution in tofu and application of $T_{[sb]}2/[s]$ relaxation measurements in determination of Tofu's water-holding capacity. *J Agr Food Chem.* (2014) 62:8594–601. doi: 10.1021/jf503427m
 23. Felby C, Thygesen LG, Kristensen JB, Jrgensen H, Elder T. Cellulose-water interactions during enzymatic hydrolysis as studied by time domain NMR. *Cellulose.* (2008) 15:703–10. doi: 10.1007/s10570-008-9222-8
 24. Tang HR, Godward J, Hills B. The distribution of water in native starch granules—a multinuclear NMR study. *Carbohydr Polym.* (2000) 43:375–87. doi: 10.1016/S0144-8617(00)00183-1
 25. Liu Y, Zhao Y, Feng X. Exergy analysis for a freeze-drying process. *Appl Thermal Eng.* (2008) 28:675–90. doi: 10.1016/j.applthermaleng.2007.06.004
 26. Molle V, Fujita M, Jensen ST, Eichenberger P, Losick R. The spo0A regulon of *Bacillus subtilis*. *Mol Microbiol.* (2004) 50:1683–701. doi: 10.1046/j.1365-2958.2003.03818.x
 27. Fujita M, Gonzalez-Pastor JE, Losick R. High- and low-threshold genes in the Spo0A regulon of *Bacillus subtilis*. *J Bacteriol.* (2005) 187:1357–68. doi: 10.1128/JB.187.4.1357-1368.2005
 28. Fimlaid KA, Shen A. Diverse mechanisms regulate sporulation sigma factor activity in the firmicutes. *Curr Opin Microbiol.* (2015) 24:88–95. doi: 10.1016/j.mib.2015.01.006
 29. Velmourougane K, Prasanna R, Saxena AK. Agriculturally important microbial biofilms: Present status and future prospects. *J Basic Microbiol.* (2017) 57:548–73. doi: 10.1002/jobm.201700046
 30. Mohsin MZ, Omer R, Huang J, Mohsin A, Zhuang Y. Advances in engineered *Bacillus subtilis* biofilms and spores, and their applications in bioremediation, biocatalysis, and biomaterials. *Syn Syst Biotechnol.* (2021) 6:180–91. doi: 10.1016/j.synbio.2021.07.002
 31. Ratti C. Hot air and freeze-drying of high-value foods: a review. *J Food Eng.* (2001) 49:311–9. doi: 10.1016/S0260-8774(00)00228-4
 32. Witrowa-Rajchert D, Lewicki PP. Rehydration properties of dried plant tissues. *Int J Food Sci Technol.* (2006) 41:1040–6. doi: 10.1111/j.1365-2621.2006.01164.x
 33. Ciurzyńska A, Lenart A. Freeze-drying-application in food processing and biotechnology—a review. *Pol J Food Nutr Sci.* (2011) 61:3. doi: 10.2478/v10222-011-0017-5